Fabrication of N-doped Carbon Coated $CoFeS_2$ Anchored rGO Nanosheet Composites: A Twin Carbon Design for Li-ion Storage and High Energy Density Supercapacitor Applications

Johnbosco Yesuraj [a#], Perumal Naveenkumar [b#], Munisamy Maniyazagan [c], Hyeon-Woo Yang [b, c], Sun-Jae Kim [b, c ,*], and Kibum Kim [a, **]

[a] *Department of Mechanical Engineering, Chungbuk National University, Cheongju 28644, Republic of Korea*

[b] *Metal-organic Compounds Materials Research Center, Sejong University, 209, Neungdong-ro, Gwangjin-gu, Seoul, 05006, Republic of Korea*

[c] *Department of Nanotechnology and Advanced Materials Engineering, Sejong University, 209, Neungdong-ro, Gwangjin-gu, Seoul, 05006, Republic of Korea*

**Corresponding author - kimkb11@chungbuk.ac.kr (Prof. Kibum Kim)

Department of Mechanical Engineering, Chungbuk National University, Cheongju 28644, Republic of Korea

*Corresponding author - sjkim1@sejong.ac.kr (Prof. Sun-Jae Kim)

Department of Nanotechnology and Advanced Materials Engineering, Sejong University, 209, Neungdong-ro, Gwangjin-gu, Seoul, 05006, Republic of Korea

[#] *These authors equally contributed to this work*

Contents

1. Materials

Cobalt nitrate hexahydrate ($Co(NO_3)_2.6H_2O$, 98%, AR), iron nitrate nonahydrate ($Fe(NO_3)_2.9H_2O$, 99%, AR), trimesic acid ($C_9H_6O_6$, 95% AR), dimethyl formamide, rGO nanosheets, sulfur powder (99.5%, AR), dopamine hydrochloride ($C_8H_{11}NO_2.HCl$, 98% AR), sodium carboxymethyl cellulose, and Acetylene black were purchased from Junsei Chemicals, South Korea.

2. Materials characterization

For TGA analysis, the samples were finely ground using a mortar and pestle. A 5 mg sample was loaded into the crucible, and the TGA analysis was recorded. For XRD analysis, the powdered sample was then spread evenly onto a sample holder or pressed into a pellet to ensure a smooth surface. The prepared sample was placed in the XRD instrument, and the diffraction pattern was recorded. For Raman analysis, a small amount of the sample was gently pressed to form a flat surface, minimizing scattering effects. The prepared sample was then positioned under the Raman microscope, and spectra were recorded using an appropriate laser source. For XPS analysis, the sample was finely ground and deposited onto a conductive substrate or pressed into a pellet to ensure a uniform surface. It was then mounted onto the sample holder, avoiding contamination and ensuring proper adhesion. The prepared sample was placed in the XPS chamber under vacuum, and the spectra were recorded. For SEM analysis, the sample was placed on a carbon tape. It was then coated with a thin layer of gold to prevent charging effects. The prepared sample was loaded into the SEM chamber, and imaging was performed under a suitable accelerating voltage. For TEM analysis, the sample was dispersed in ethanol and ultrasonicated for 20 minutes to achieve a uniform suspension. A few drops of the dispersion were placed onto a carbon-coated copper grid (200 mesh) and allowed to dry. The prepared grid was then loaded into the TEM chamber for imaging under high-resolution conditions. With a LECO CHNS-932 analyzer, elemental chemical analysis (ECA) was used to quantitatively determine the C, H, N, S, and O contents of all samples. Usually, 1 mg of the material was put in an Ag crucible and burned at 1333 K in an environment of pure oxygen.

3. Lithium-ion battery anode characterizations

The coating ink was prepared by mixing the active materials ($CoFeS_2$, $CoFeS_2$@rGO, and $CoFeS_2$@rGO/N-C), conductive carbon black, and sodium carboxymethyl cellulose (7:2:1 ratio) in an aqueous solution. The pre-cleaned Cu foil was used as the current collector and the coating ink was uniformly applied to it using the doctor blade method. At 80°C, the coated electrodes were dried for 12 hours in a vacuum oven. The obtained electrode was then transferred to an argon-filled glove box, where 12 mm diameter circular electrodes were punched for the assembly of a 2032 coin cell. The loaded active mass of the electrode materials is 1.19 mg cm^{-2}, 1.19 mg cm^{-2}, and 1.19 mg cm^{-2} of $CoFeS_2$, $CoFeS_2$@rGO, and $CoFeS_2$@rGO/N-C composite. The working electrode, a circular lithium foil counter electrode, a Celgard 2300 separator, and an electrolyte made of 1.2 M $LiPF_6$ (100 μL) in a solution of ethylene and dimethyl carbonates with 3 wt% vinylene carbonate were used to fabricate the 2032-coin cell. A Biologic workstation (model-VMP3) instrument was employed to record cyclic voltammetry (CV), and electrochemical impedance spectroscopy (EIS) analysis. The CV tests were performed using a potential window from 0.01 to 3.0 V at various scan rates, while EIS was measured over a frequency range of 0.1 kHz to 100 MHz with an amplitude of 5 mVs^{-1}. The cyclic performance (at 1 Ag^{-1}) and rate capability studies were evaluated by the WonAtech battery tester (WBCS3000S) within the voltage window of 0.01 to 3.0 V. In a lithium-ion battery, before the cyclic test, the cells were cycled up to 10 cycles at a low current density of 100 mA g^{-1} for the activation process.

4. Supercapacitor analysis

Supercapacitor performances of $CoFeS_2$, $CoFeS_2$@rGO, and $CoFeS_2$@rGO/N-C were evaluated using both three-electrode and two-electrode asymmetric device configurations on a ZIVE LAB SP-10 electrochemical workstation. The active material (80 %), carbon black (10 %), and polyvinylidene difluoride (10 %) binder were mixed in N-Methyl-2-pyrrolidone (NMP) solvent. The mixture was ground into a slurry using a mortar and pestle and then brush-coated onto pre-cleaned nickel foam (1 cm ×1 cm). The NMP solvent in coated electrodes was evaporated at 80 °C for 6 hours in a vacuum oven. The active mass of each electrode was approximately 3.7 mg. When calculating gravimetric capacitance, only the active material weight is considered, excluding the conducting carbon and binder. In the three-electrode configuration, CV, GCD, and EIS were utilized to analyze the supercapacitor properties. A 2 M KOH solution served as the aqueous electrolyte solution, with a Hg/HgO electrode as the reference, platinum foil as the counter electrode, and the active material-coated Ni-foam current collector as the active working electrode.

For asymmetric device (ASC) fabrication, activated carbon (AC)-coated Ni-foam and $CoFeS_2$@rGO/N-C coated Ni-foam were employed as the negative and positive electrodes respectively. The AC electrode was constructed by combining activated carbon and PVDF binder in a 90:10 ratio with NMP solvent. The resultant coating ink was brush-coated onto nickel foam and dried at 80°C for 6 hours in a vacuum oven. A PVA/KOH gel electrolyte was employed, with a PTFE film used as the separator. To prepare the gel electrolyte, 6 g of polyvinyl alcohol (PVA) and 3.58 g of KOH were dissolved homogeneously in 60 mL of deionized water at 90 °C with constant stirring. The ASC components were assembled by dipping all parts in the PVA/KOH gel electrolyte and sandwiching them together. The electrolyte was then allowed to air-dry within the device, completing the assembly for electrochemical testing. Calculations for charge balance, specific capacity, specific capacitance, energy density, power density, and coulombic efficiency are provided in the supplemtary information, equations S 1 to S8. Before the supercapacitor analysis, all the electrodes were activated by running 50 CV cycles at a scan rate of 50 mV s^{-1}.

5. Equations

To conquer the superior electrochemical features of the ASC device, the charge is balanced between the positive and negative electrodes employing the following equations (S 1) and (2).

$$Q_{+} = Q_{-} \qquad \text{(S 1)}$$

$$\frac{m_{+}}{m_{-}} = \frac{C_{-} \times \Delta V_{-}}{C_{+} \times \Delta V_{+}} \qquad \text{(S 2)}$$

Here, m_+ and m_-; C_+ and C_-; and ΔV_+ and ΔV_- signify the weight of active electrode materials, specific capacitance from the CV analysis at 50 mV s$^{-1,}$ and voltage window of the positive and negative electrodes, respectively. The specific capacitance values (F g^{-1}) from the CV curves of the anode and cathode were calculated using Equation (S 3).

$$Csp = \frac{\int IdV}{SmV}, \qquad \text{(S 3)}$$

where I refers to the maximum current density of CV curves V denotes the potential window of the CV curves, m represents electrode material weight and S refers the sweep rate correspondingly. The specific capacity (C_s), specific capacitance (C_{sp}), energy density (E_{cell}) (WhKg^{-1}), and power density (P_{cell}) (WKg^{-1}) values were assessed by the Equations S (4-7), respectively.

$$C_s = \frac{I \times \Delta t}{3.6 \times m} \quad \text{(S4)}$$

$$C_{sp} = \frac{I \times \Delta t}{m \times \Delta V} \quad \text{(S5)}$$

$$E_{cell} = \frac{1}{2 \times 3.6} \times C_{sp} \times \Delta V^2 \quad \text{(S6)}$$

$$P_{cell} = \frac{3600 \times E_{cell}}{\Delta t} \quad \text{(S7)}$$

where I, Δt, m, and ΔV represent the input current density, discharge time from the GCD curves, active electrode material weight, and voltage window respectively.

The coulombic efficiency (η) is calculated using Equation (S8) :

$$\eta = {}^{t_D}\!/_{t_C} \times 100 \quad (S8)$$

where t_D and t_C Are discharging and charging time, respectively?

6. XPS analysis

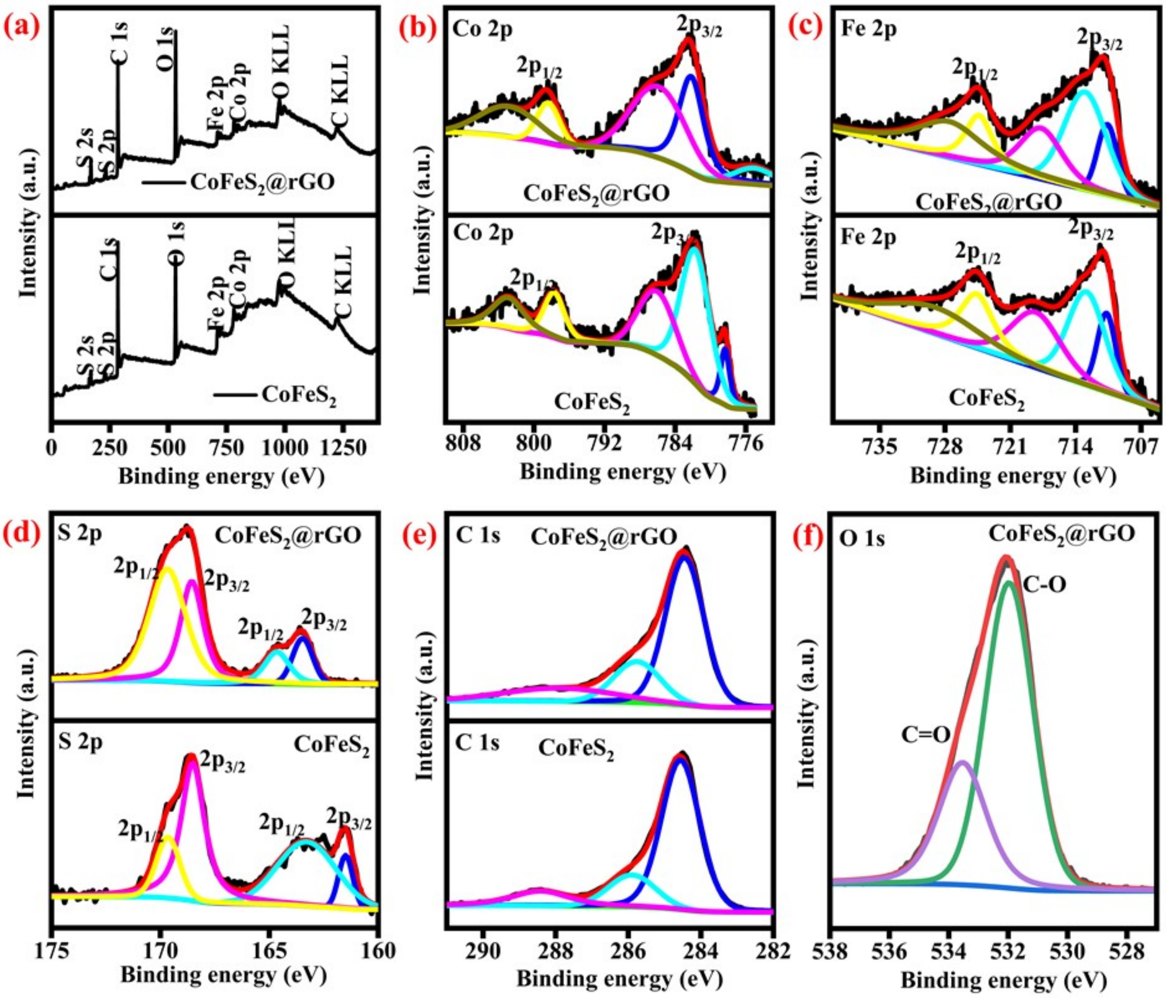

Figure S1 The XPS results of (a) Survey spectrum, (b) Co 2p, (c) Fe 2p, (d) S 2p, and (e) C 1s of $CoFeS_2$ and $CoFeS_2$@rGO materials, and (f) O 1s orbitals of $CoFeS_2$@rGO materials.

Table S1 Compassion of obtained binding energy values of elements in $CoFeS_2$, $CoFeS_2$@rGO, and $CoFeS_2$@rGO/N-C materials.

Elements	**$CoFeS_2$**	**$CoFeS_2$@rGO**	**$CoFeS_2$@rGO/N-C**
Co 2p	778.41 eV (Co^{3+})	775.48 eV (Co^{3+})	778.23 eV (Co^{3+})
	781.96 eV (Co^{2+})	782.21 eV (Co^{2+})	781.02 eV (Co^{2+})
	786.29 eV(satellite)	786.34 eV(satellite)	785.62 eV (satellite)

	797.68 eV (Co^{2+}) 803.08 eV (satellite)	798.50 eV (Co^{2+}) 803.08 eV (satellite)	794.06 eV (Co^{3+}) 802.94 eV (satellite)
Fe 2p	710.65 eV (Fe^{2+}) 712.95 eV (Fe^{3+}) 718.46 eV (satellite) 724.58 eV (Fe^{2+}) 729.40 eV (Fe^{3+})	710.72 eV (Fe^{2+}) 713.72 eV (Fe^{3+}) 717.88 eV (satellite) 724.33 eV (Fe^{2+}) 727.73 eV (Fe^{3+})	710.46 eV (Fe^{2+}) 715.09 eV (Fe^{3+}) 722.96 eV (Fe^{2+}) 726.46 eV (Fe^{3+})
S 2p	161.47 eV (S^{2-}) 163.32 eV (S^{2-}) 168.50 eV (SO_4^{2-}) 169.62 eV(SO_4^{2-})	163.50 eV (S^{2-}) 164.64 eV (S^{2-}) 168.50 eV (SO_4^{2-}) 169.64 eV (SO_4^{2-})	161.40 eV (S^{2-}) 163.70 eV (S^{2-}) 168.2 eV (SO_4^{2-}) 169.20 eV (SO_4^{2-})
C 1s	284.55 eV (C-C/C=C) 285.92 eV (C-O) 288.42 eV(C=O)	284.45 eV (C-C/C=C) 285.78 eV (C-O) 288.07 eV (C=O)	284.73 eV (C-C/C=C) 286.24 eV(C-O/C-N) 288.43 eV(C=O)
O 1s	---	531.98 eV(C-O) 533.54 eV (C=O)	531.51 eV (C-O) 534.51 eV(C=O)
N 1s	---	---	398.40 eV (pyridine N) 400.32 eV (pyrrolic N) 403.08 eV (graphitic N)

Table S2 Atomic percentage of elements in $CoFeS_2$, $CoFeS_2$@rGO, and $CoFeS_2$@rGO/N-C materials as determined by XPS analysis

Elements	$CoFeS_2$	$CoFeS_2$@rGO	$CoFeS_2$@rGO/N-C
Fe	2.65	1.89	1.36
Co	3.44	2.17	1.28
S	7.36	6.31	6.40
C	86.54	59.30	73.24

O	---	30.33	12.89
N	--	---	4.82

7. CHNS analysis

Table S3 Summary of C, N, S, and O elements in $CoFeS_2$, $CoFeS_2$@rGO, and $CoFeS_2$@rGO/N-C materials.

Elements	**$CoFeS_2$**	**$CoFeS_2$@rGO**	**$CoFeS_2$@rGO/N-C**
C	14.20 %	16.81 %	22.40 %
S	28.65 %	18.87 %	20.7 %
N	---	---	1.33 %
O	---	27.93 %	19.73 %

8. Morphological and EDS analysis of $CoFeS_2$

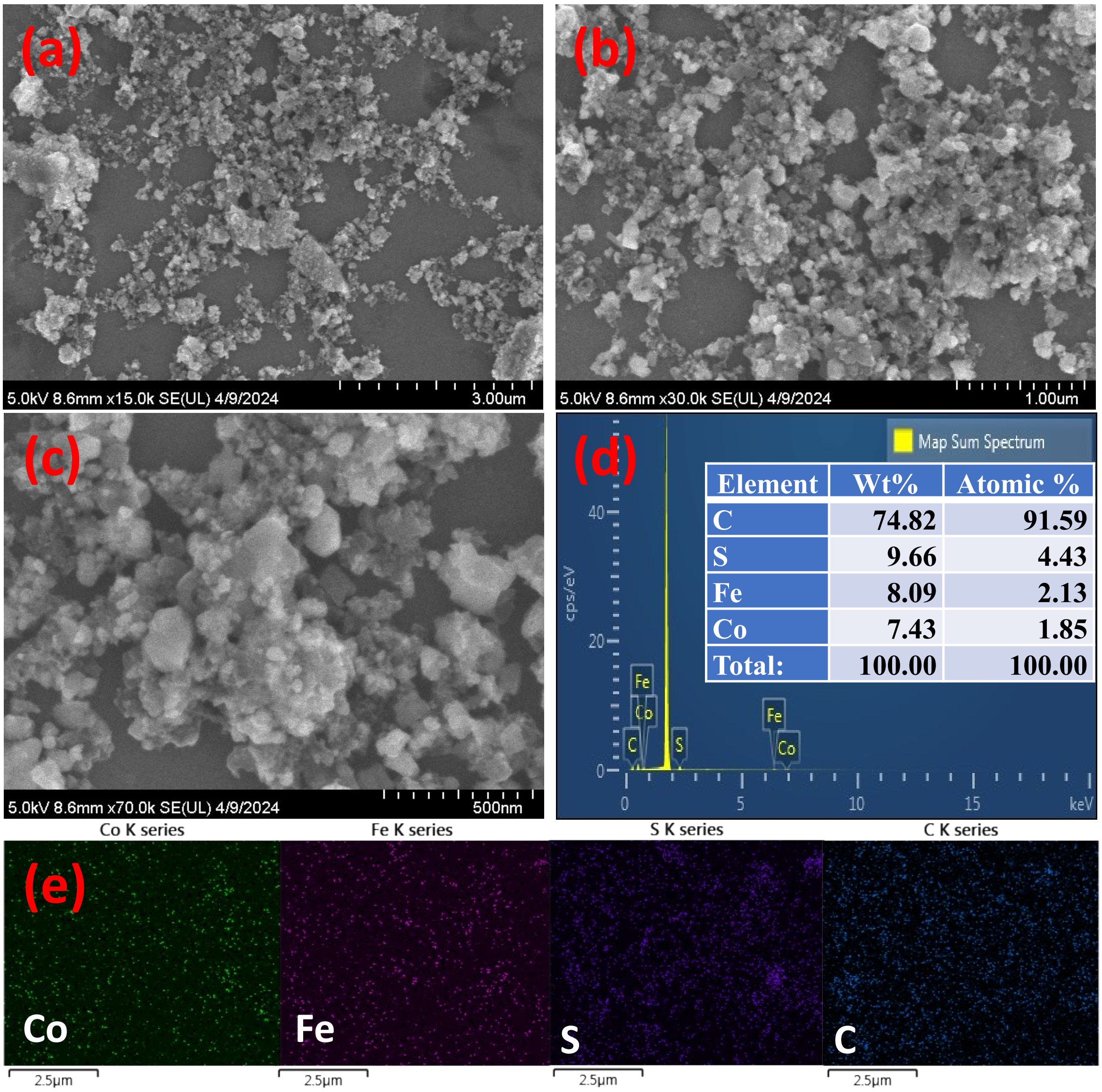

Element	Wt%	Atomic %
C	74.82	91.59
S	9.66	4.43
Fe	8.09	2.13
Co	7.43	1.85
Total:	100.00	100.00

Figure S2 (a-c) HR-SEM images, (d) EDS spectrum with elements atomic percentage table, and (e) mapping results of elements of $CoFeS_2$ materials.

9. The d-spacing and EDS analyses of $CoFeS_2$@rGO material

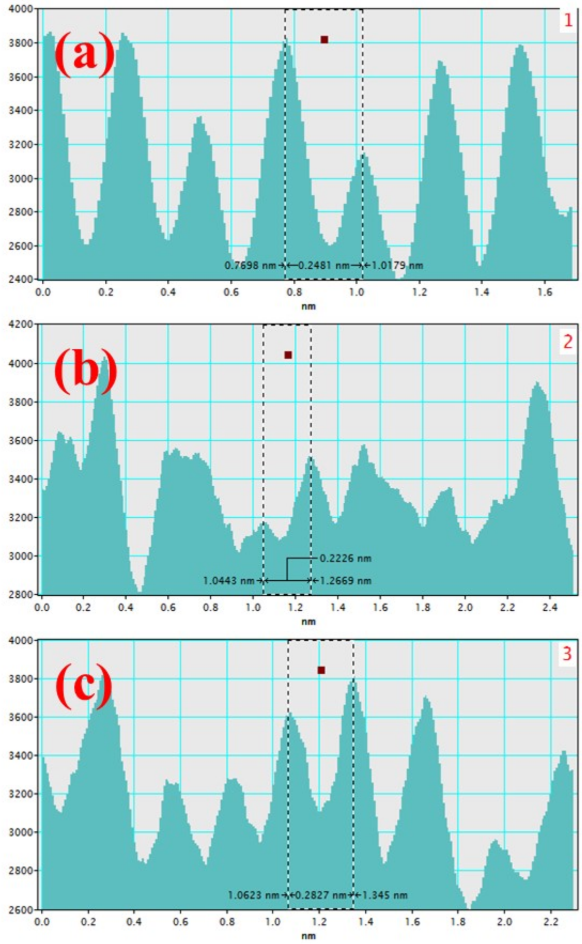

Figure S3 (a-c) d-spacing spectrum of $CoFeS_2$@rGO material from the HR-TEM results.

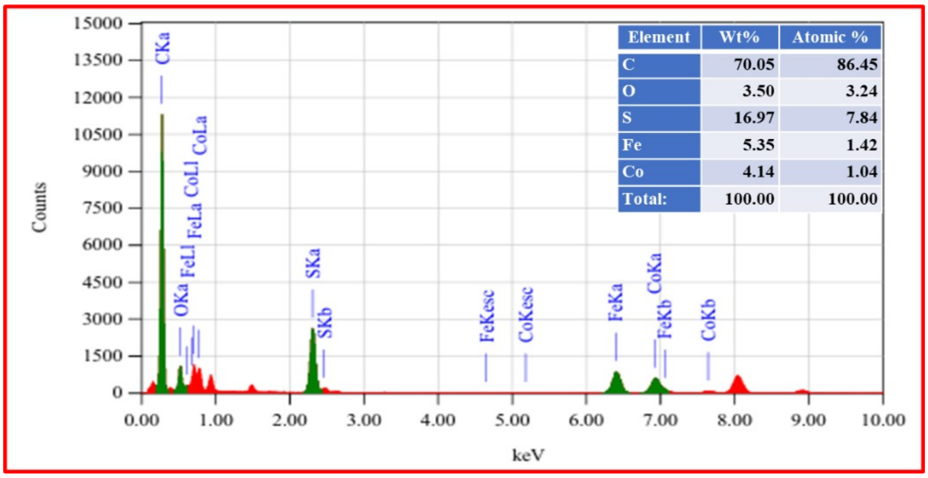

Element	Wt%	Atomic %
C	70.05	86.45
O	3.50	3.24
S	16.97	7.84
Fe	5.35	1.42
Co	4.14	1.04
Total:	100.00	100.00

Figure S 4: EDS analysis of $CoFeS_2$@rGO material

10. The d-spacing analysis of $CoFeS_2$@rGO/N-C material

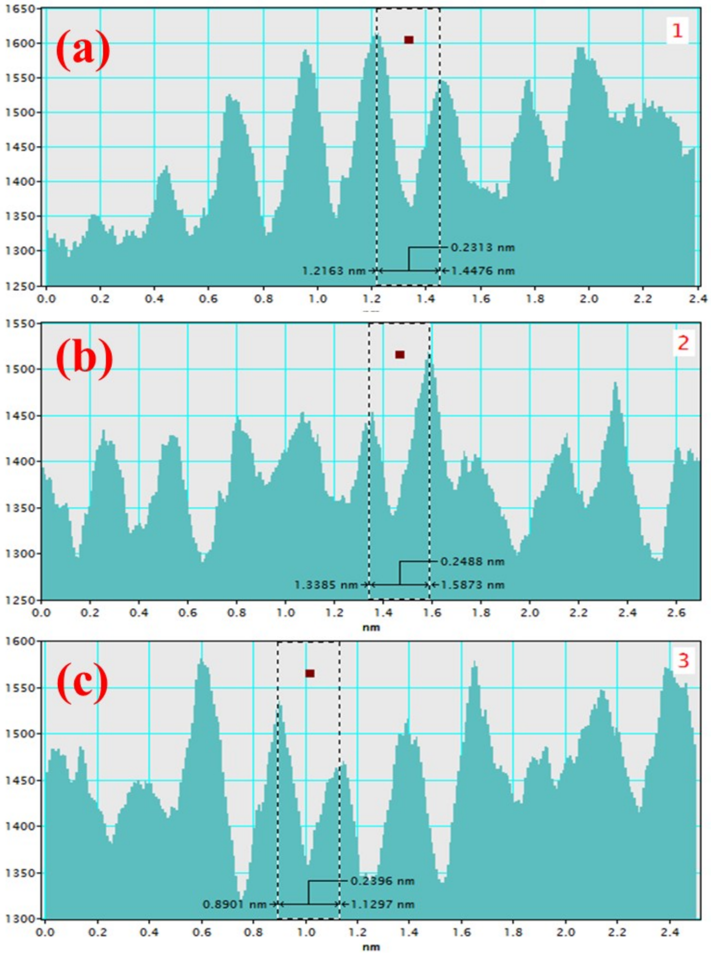

Figure S5 (a-c) d-spacing spectrum,

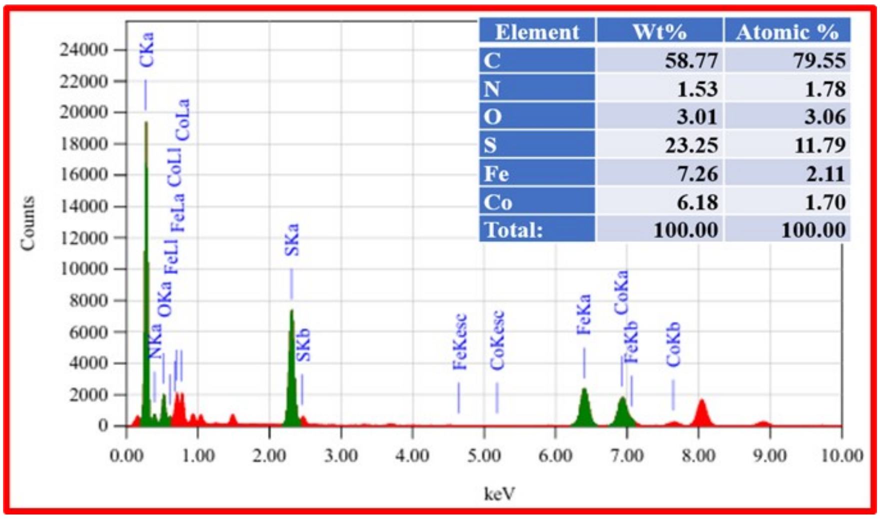

Element	Wt%	Atomic %
C	58.77	79.55
N	1.53	1.78
O	3.01	3.06
S	23.25	11.79
Fe	7.26	2.11
Co	6.18	1.70
Total:	100.00	100.00

Figure S 6: EDS spectrum with elements atomic percentage table of $CoFeS_2$@rGO/N-C material.

11. BET surface analysis

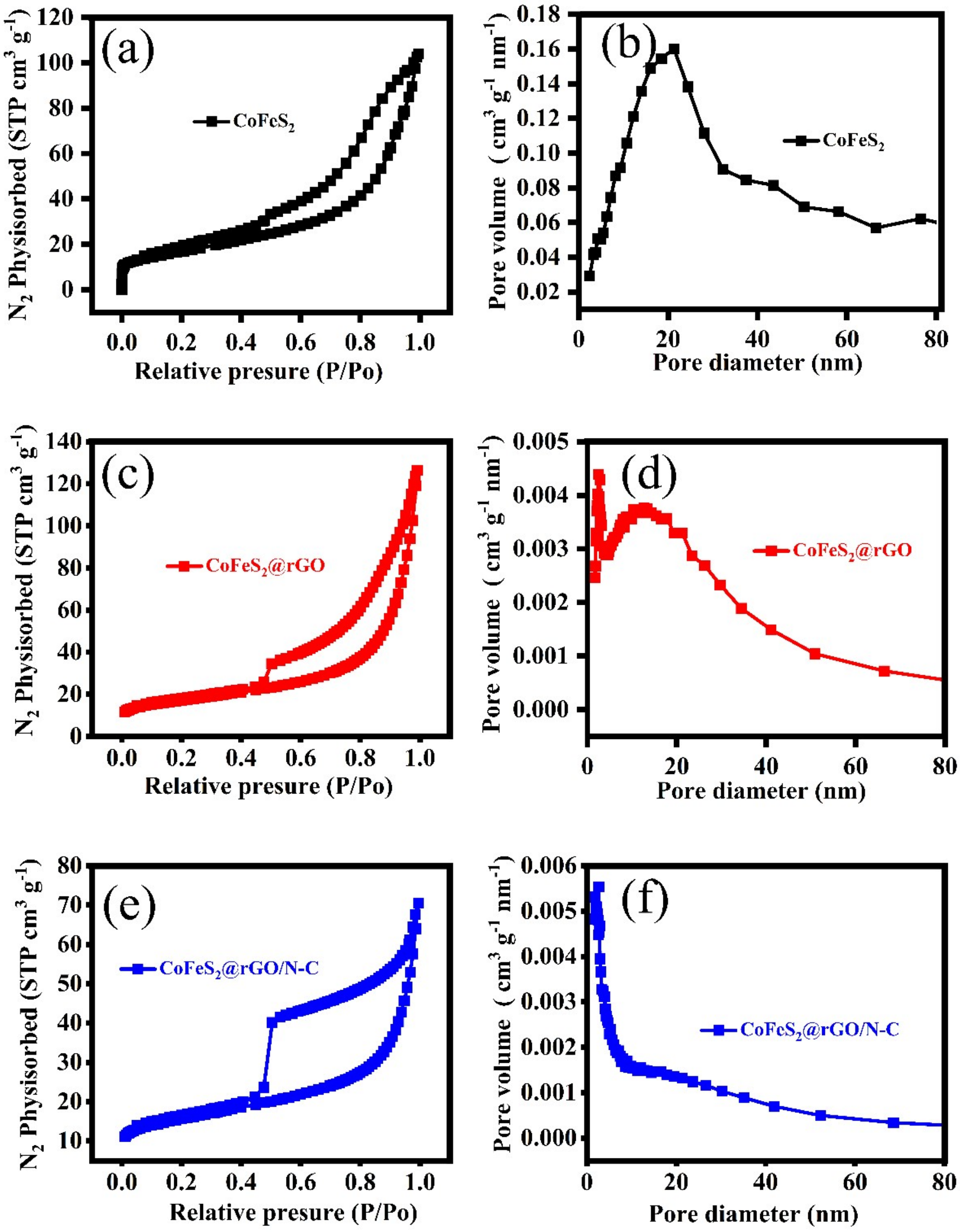

Figure S7 (a, c, & e) N_2 adsorption/desorption plot and (b, d, & f) pore size distributions plot of $CoFeS_2$, $CoFeS_2$@rGO, and $CoFeS_2$@rGO/N-C materials.

12. Post-electrochemical studies

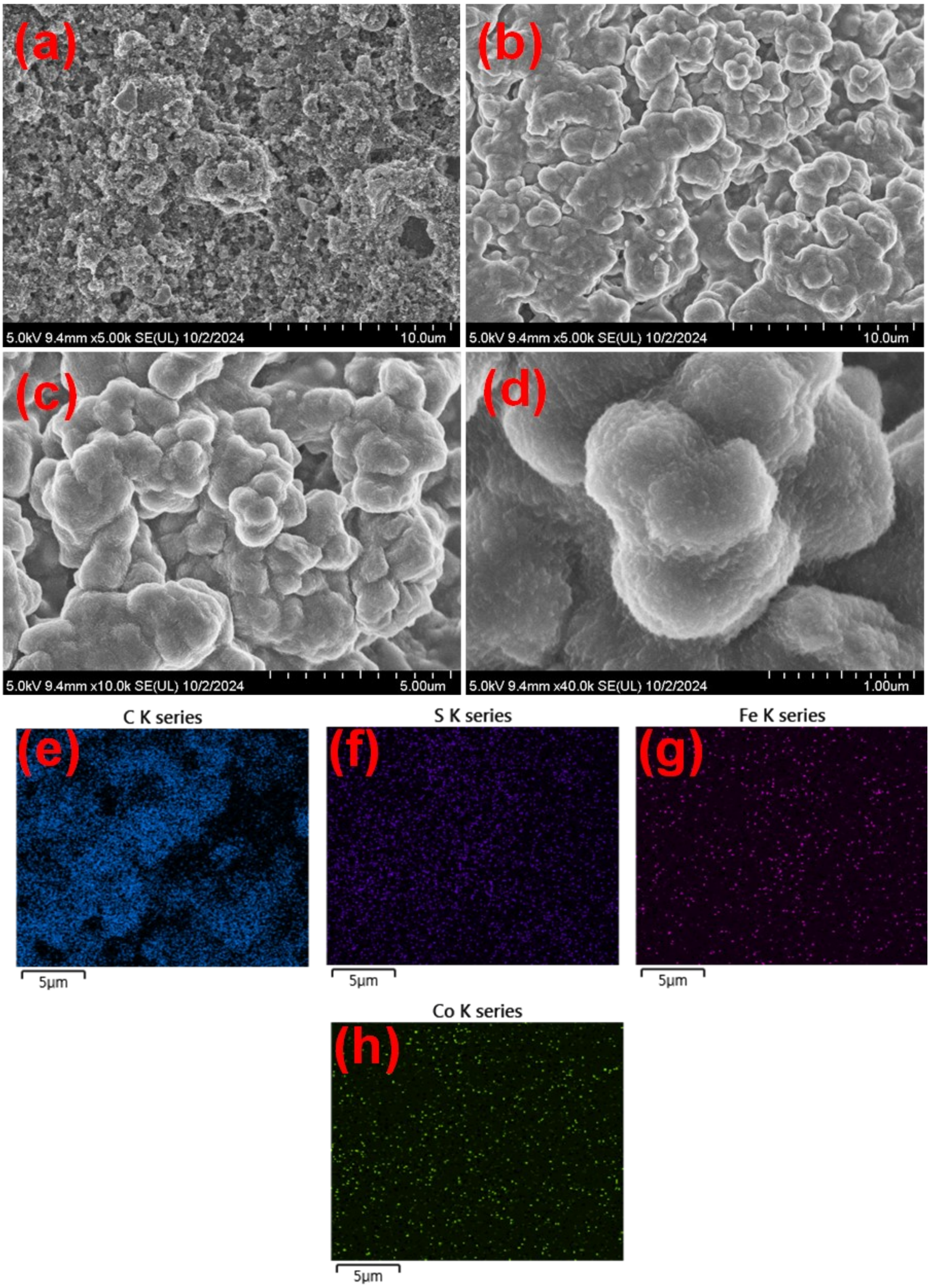

Figure S8: SEM images of (a) fresh electrode and (b-d) tested $CoFeS_2$ electrode after 1000th cycle at 1 A g^{-1} and Elemental mapping results of (e-f) C, S, Fe and Co elements.

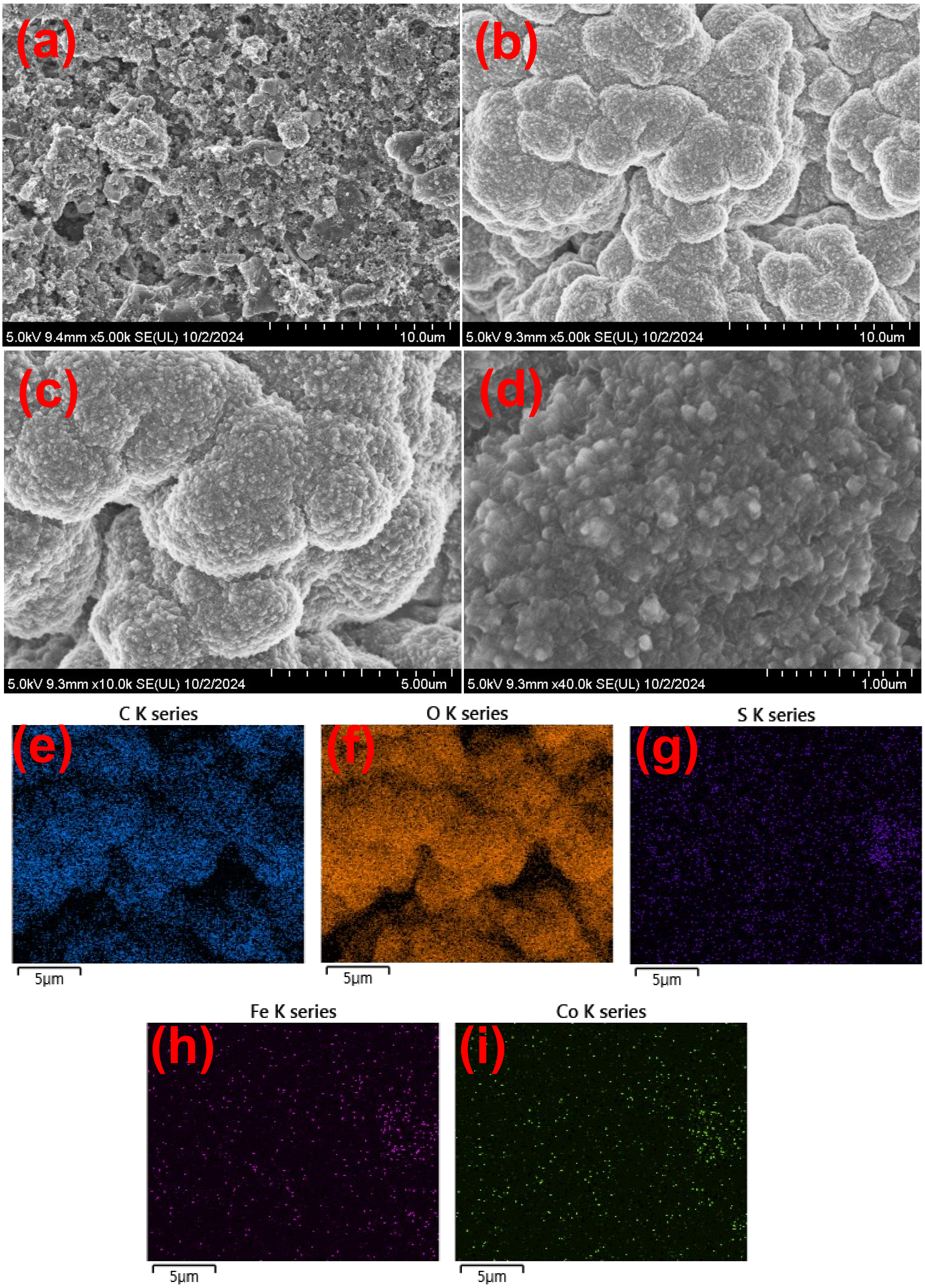

Figure S9: SEM images of (a) fresh electrode and (b-d) tested $CoFeS_2$@rGO electrode after 1000th cycle at 1 A g^{-1} and Elemental mapping results of (e-f) C, O, S, Fe and Co elements.

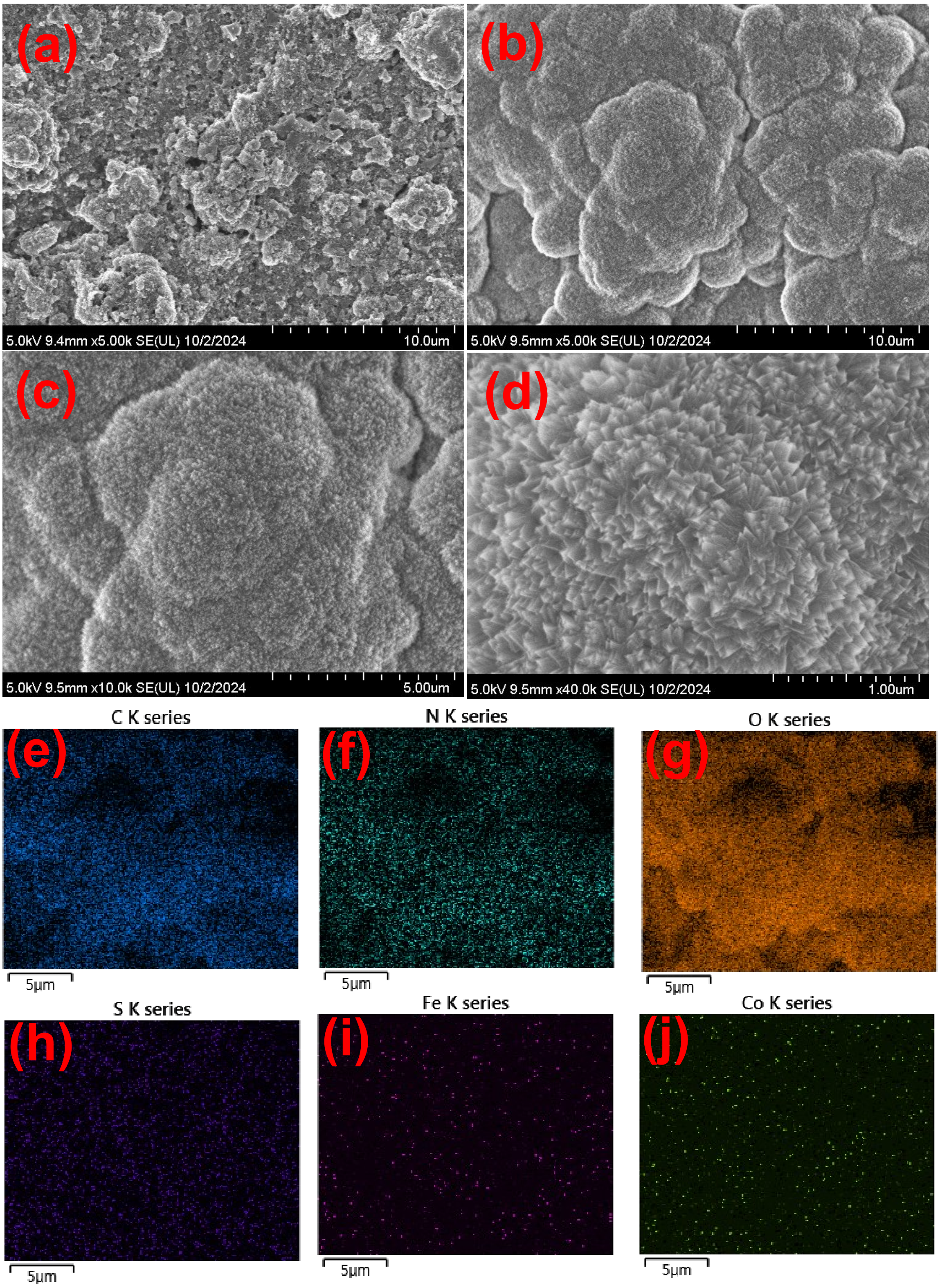

Figure S10: SEM images of (a) fresh electrode and (b-d) tested $CoFeS_2$@rGO/N-C electrode after 1000th cycle at 1 A g^{-1} and Elemental mapping results of (e-f) C, N, O, S, Fe and Co elements.

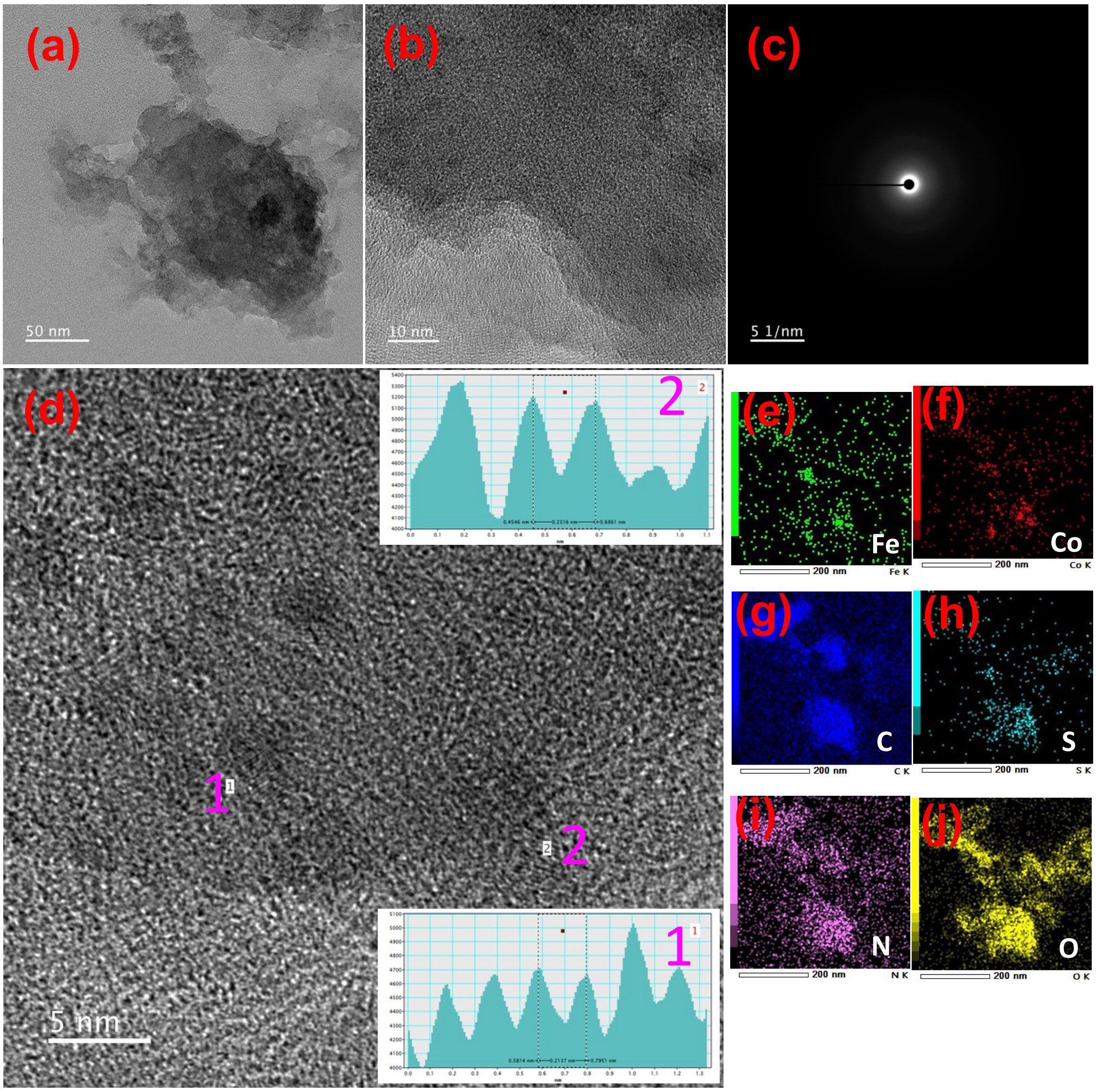

Figure S11: HR-TEM images of (a-d) tested $CoFeS_2$@rGO/N-C electrode after 1000th cycle at 1 A g^{-1} , (d) inert figure – lattice fringes and (e-j) Elemental mapping results of Fe, Co, C, S, N, and O elements.

13. Equations for surface-controlled reaction

Reaction mechanism for the surface-controlled process, depicted in equation S (8-11) [1]

$$CoFeS_2 + 2OH^- \rightleftharpoons FeSOH + CoSOH + 2e^- \quad \text{(S8)}$$

$$CoSOH + OH^- \rightleftharpoons CoSO + H_2O + e^- \quad \text{(S9)}$$

$$FeSOH + OH^- \rightleftharpoons FeSO + H_2O + e^- \quad \text{(S10)}$$

14. Floating test

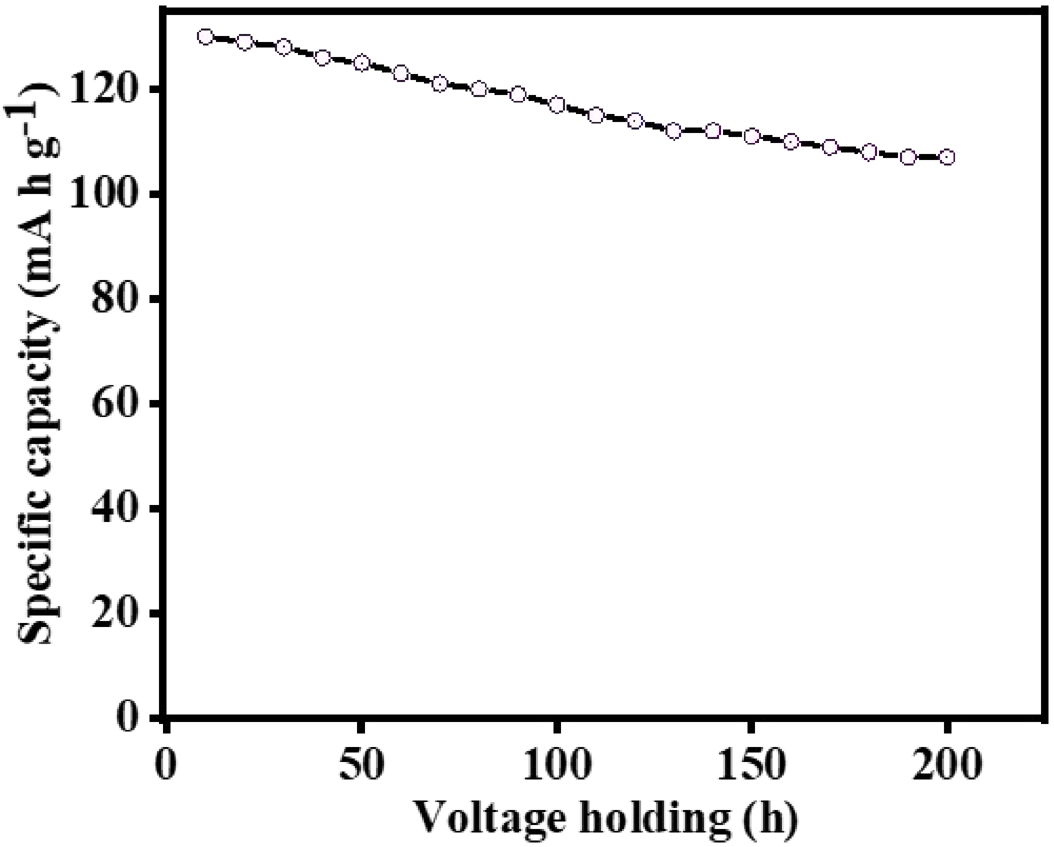

Figure S 12: Floating test for $CoFeS_2$@rGO/N-C//activated carbon asymmetric device

15. Post studies

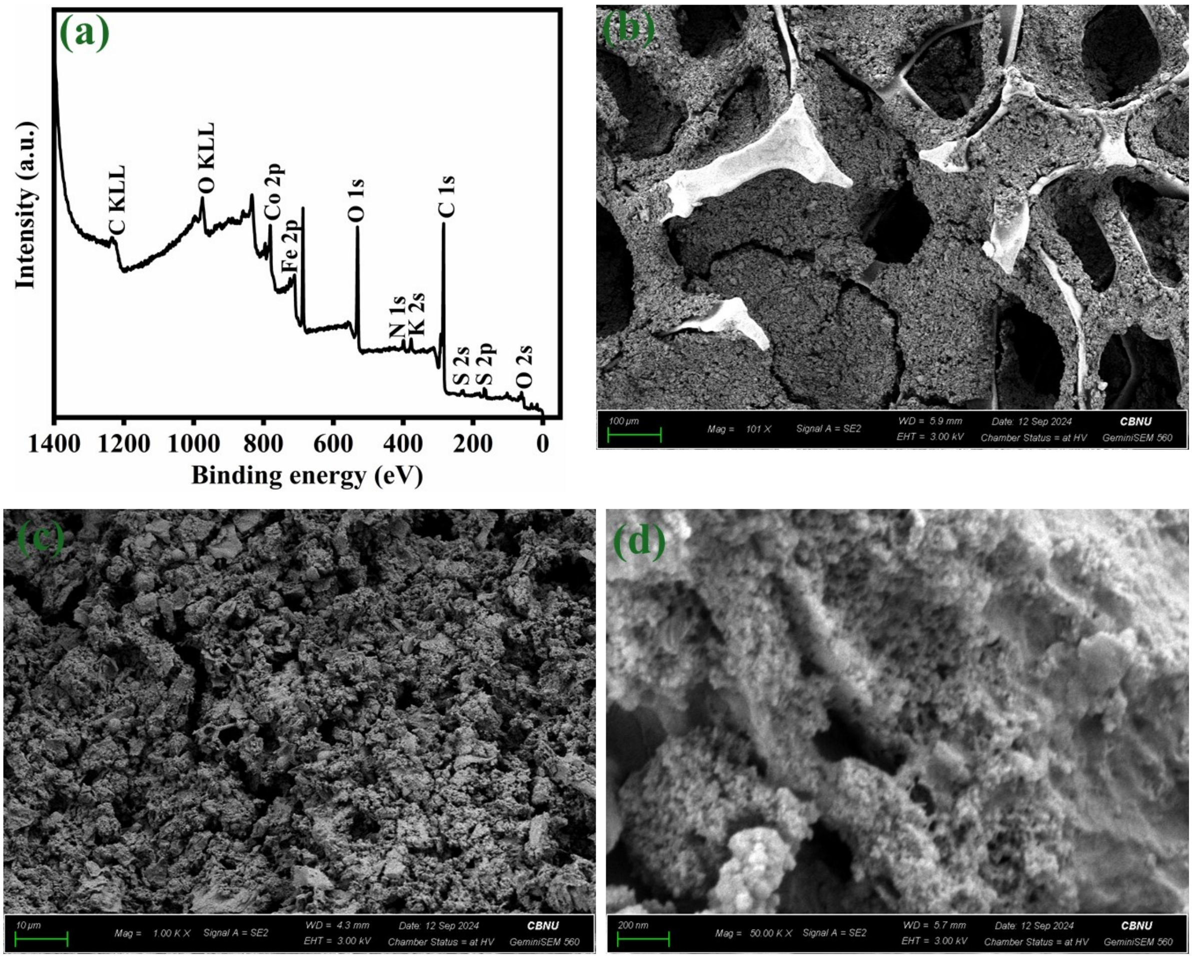

Figure S13: (a) Survey spectrum, (b-d) SEM analysis of $CoFeS_2$@rGO/N-C after cyclic stability analysis.

References

[1] M. Shirvani, S.S. Hosseiny Davarani, Designing of the CoFeX (X= Se, P, S) Flower-like Structures on Nickel Foam as Efficient Positive Electrodes for a High-Performance Hybrid Supercapacitor, Energy and Fuels. 37 (2023) 9626–9640. https://doi.org/10.1021/acs.energyfuels.3c00975.